Finite element modeling of interactions between pelvic organs due to pressure

Zhuowei Chen, Pierre Joli, Zhi-Qiang Feng

CSMA 2011
10e Colloque National en Calcul des Structures
9-13 Mai 2011, Presqu'île de Giens (Var)

Finite element modeling of interactions between pelvic organs due to pressure

Z.W. Chen[1], P. Joli[1], Z.-Q. Feng[1]

[1] *LME-Evry, Université d'Evry/PRES Universud Paris, 40 rue de Pelvoux, 91020 Evry, France, {chen, pjoli, feng}@iup.univ-evry.fr*

Résumé — Pelvic floor (pelvic support) disorders occur only in women and become more common as women age. However, the surgical practices remain poorly evaluated. The realization of a simulator of the dynamic behavior of the pelvic organs is an identified need. To determine the strain and stress in the biological soft tissues hyperelastic constitutive laws are often used in the context of finite element analysis. In our work, the Mooney-Rivlin model was taken into consideration to simulate the interactions between these organs due to pressure.
Mots clés — Pelvic organs, hyperelastic, finite element, interactions, Mooney-Rivlin model, pressure.

1 Introduction

Pelvic floor (pelvic support) disorders occur only in women and become more common as women age. They involve a dropping down (prolapse) of the bladder, urethra, small intestine, rectum, uterus, or vagina caused by the failure of the system of support. About 11.1%of women need surgery for a pelvic floor disorder during her lifetime, given an average life expectancy is 79 years[1]. However, the surgical practices remain poorly evaluated. The realization of a simulator of the dynamic behavior of the pelvic organs which allowing the surgeon to estimate the functional impact of his actions before his implementation is then a need identified.

Our project is to conceive a simulator of soft tissues based on physical behaviours of each organ taking into account interactions between them inside the pelvic cavity. This simulator will be in a loop of a clinical routine to provide preoperative information for the surgery planning. In this workflow, the simulation will be based on a patient-specific in which each geometrical model will be carried out starting from MRI acquisition of pelvic organs of one patient as shown in Figure 1[2]. The constraint time simulation has to be considered and fast computational methods are necessary to solve large deformations with multiple contacts.

From a mechanical point of view, the pelvic organs have specific geometries and material properties. They can be thought of as biomechanical structures move and interact with each other, due to the external pressures, while the constraints are induced by rigid bodies (bones) as well as soft tissues such as muscles, ligaments and fascias, all ensuring the stability of these organs.

2 Goemetrical definition of the pelvic system

A geometrical rebuilding is performed based on the magnetic resonance image (MRI) data from a single patient without genital prolapse. However, there is a problem meshing the 3D model, so as the first step of this work, a 2D sagittal section of the 3D model was chosen to be the test model. The mesh is constructed with plane quadrilateral elements.

3 Mechanical properties and constitutive laws

The characterisation of the mechanical behaviour of pelvic tissues is an essential step for performing the numerical simulation. The biological soft tissues are often considered as non-linear elastic, large deformation and quasi-incompressible materials[3]. To determine the strain and stress in the biological soft

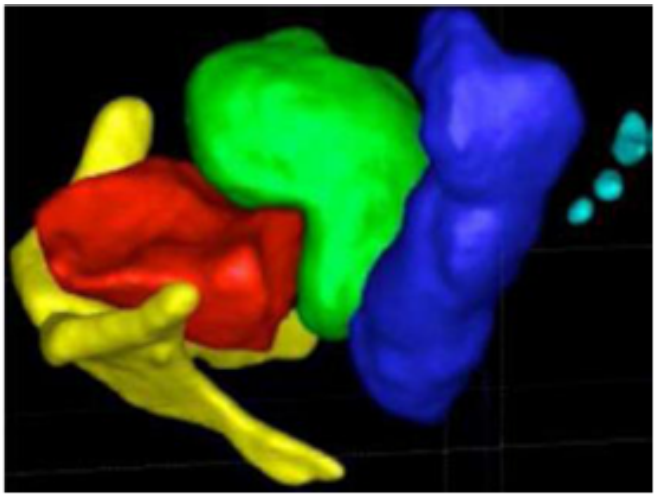

FIGURE 1 – Geometrical models of pelvic organs

tissues such as ligaments, tendons, pelvic organs or arterial walls, anisotropic hyperelastic constitutive laws are often used in the context of finite element analysis.

Among the different strain energy density functions available in the literature, Mooney-Rivlin is often chosen in the simulation of organs' contact[4]. Usually, the hyperelastic materials undergo large deformations. In order to describe the geometrical transformation problems, the deformation gradient tensor is introduced by

$$F_{ij}(\mathbf{x}) = \delta_{ij} + \frac{\partial u_i}{\partial u_j} \quad \text{or} \quad \mathbf{F} = \mathbf{I} + \nabla \mathbf{u} \tag{1}$$

where $\mathbf{I}$ is the unity tensor, $\mathbf{x}$ the position vector and $\mathbf{u}$ the displacement vector. Because of large displacements and rotations, Green-Lagrangian strain is adopted for the non-linear relationships between strains and displacements. We note $\mathbf{C}$ the stretch tensor or the right Cauchy-Green deformation tensor ($\mathbf{C} = \mathbf{F}^{\mathbf{T}}\mathbf{F}$). The Green-Lagrangian strain tensor $\mathbf{E}$ is defined by

$$\mathbf{E} = (\mathbf{C} - \mathrm{I})/2 \tag{2}$$

In the case of hyperelastic law, there exists an elastic potential function W (or strain energy density function) which is a scale function of one of the strain tensors, whose derivative with respect to a strain component determines the corresponding stress component. This can be expressed by

$$\mathbf{S} = \frac{\partial W}{\partial \mathbf{E}} = 2\frac{\partial W}{\partial \mathbf{C}} \tag{3}$$

where $\mathbf{S}$ is the second Piola-Kirchoff stress tensor. In the particular case of isotropic hyperelasticity, (3) can be written by

$$\mathbf{S} = 2\left[I_3 \frac{\partial W}{\partial I_3}\mathbf{C}^{-1} + \left(\frac{\partial W}{\partial I_1} + I_1 \frac{\partial W}{\partial I_2}\right)\mathbf{I} - \frac{\partial W}{\partial I_2}\mathbf{C}\right] \tag{4}$$

where I_i (i = 1,2,3) denote the invariants of the right Cauchy-Green deformation tensor $\mathbf{C}$:

$$I_1 = C_{ii}\ ;\ I_2 = (I_1^2 - C_{ij}C_{ij})/2\ ;\ I_3 = \det(\mathbf{C}) \tag{5}$$

In case of isotropic behaviour, the Mooney-Rivlin model, described by the strain energy density function, is often chosen in the literature to model the behaviour of the soft tissue materials. This model has been implemented into an in-house finite element code FER[5]to model the bladder, the rectum and the uterus. The Mooney-Rivlin strain energy density formulation is given by

$$W = C_{10}(I_1 - 3) + C_{01}(I_2 - 3) + \frac{1}{d}(J-1)^2 \tag{6}$$

where C_{10} , C_{01} and d are the material coefficients. I_1 and I_2 are the first and second invariants, respectively. Noticed that if d approaches infinity, the last part of equation (6) will disappear or approach zero, so it will back to strain energy density function for an incompressible Mooney-Rivlin material.

4 Loading application

The essential problem is to assign suitable loadings on the system taking into account the pelvic organs encountered in the phenomenon of prolapses. As mentioned before, these organs move and interact with each other, due to the external pressures, so we considered applying a compressive pressure exerted by the lungs onto the pelvic area.

Because of large deformations, the loading application of compressive pressure on the pelvic area is non linear and highly dependent of the current configuration of the organs. Indeed these loads are always normal to the deformed surfaces of the organs which will be considered in out work as follows.

The surface load term is given by

$$\mathbf{F}_p = \int_a p\mathbf{n}da \tag{7}$$

where p is the uniform pressure which acting on a surface a having a pointwise normal $\mathbf{n}$. In this equation the magnitude of the area element and the orientation of the normal are both deformation-dependent. In terms of parameterization the normal and area elements can be obtained in terms of the tangent vectors $\partial\mathbf{x}/\partial\xi$ and $\partial\mathbf{x}/\partial\eta$ as,

$$\mathbf{n} = \frac{\frac{\partial\mathbf{x}}{\partial\xi}\times\frac{\partial\mathbf{x}}{\partial\eta}}{\left\|\frac{\partial\mathbf{x}}{\partial\xi}\times\frac{\partial\mathbf{x}}{\partial\eta}\right\|}; \quad da = \left\|\frac{\partial\mathbf{x}}{\partial\xi}\times\frac{\partial\mathbf{x}}{\partial\eta}\right\| d\xi d\eta \tag{8}$$

The deformation-dependent load vector (7) can be transformed to the reference configuration of the loaded element surface,

$$\mathbf{F}_p = \int_a p\mathbf{n}da = \int_A p(\frac{\partial\mathbf{x}}{\partial\xi}\times\frac{\partial\mathbf{x}}{\partial\eta})d\xi d\eta \tag{9}$$

where A is the parameter plane.

The cross product in (9) can be computed as,

$$\hat{\mathbf{n}}_e = \varphi_{e,\xi}\times\varphi_{e,\eta} = \left\{\begin{array}{c} x_{2,\xi}x_{3,\eta} - x_{3,\xi}x_{2,\eta} \\ x_{3,\xi}x_{1,\eta} - x_{1,\xi}x_{3,\eta} \\ x_{1,\xi}x_{2,\eta} - x_{2,\xi}x_{1,\eta} \end{array}\right\} \tag{10}$$

The corresponding virtual work component is,

$$\delta W^p_{ext} = \int_a p\mathbf{n}\cdot\delta\mathbf{v}da \tag{11}$$

where $\delta\mathbf{v}$ denotes an arbitrary virtual velocity from the current position of the body.

Express (11) in the parameter plane as,

$$\delta W^p_{ext} = \int_A p\delta\mathbf{v}\cdot(\frac{\partial\mathbf{x}}{\partial\xi}\times\frac{\partial\mathbf{x}}{\partial\eta})d\xi d\eta \tag{12}$$

To linearize (12), after some algebraic operations[6], we can get a symmetric function,

$$\begin{array}{l} D\delta W^p_{ext}[\mathbf{u}] = \frac{1}{2}\int_A p\frac{\partial\mathbf{x}}{\partial\xi}\cdot\left[(\frac{\partial\mathbf{u}}{\partial\eta}\times\delta\mathbf{v}) + (\frac{\partial\delta\mathbf{v}}{\partial\eta}\times\mathbf{u})\right]d\xi d\eta \\ -\frac{1}{2}\int_A p\frac{\partial\mathbf{x}}{\partial\eta}\cdot\left[(\frac{\partial\mathbf{u}}{\partial\xi}\times\delta\mathbf{v}) + (\frac{\partial\delta\mathbf{v}}{\partial\xi}\times\mathbf{u})\right]d\xi d\eta \end{array} \tag{13}$$

Discretization of this equation will lead to a symmetric component of the tangent matrix, therefore, the vector of stiffness coefficients is given by

$$k_{p,ab} = \frac{1}{2}\int_A p\frac{\partial \mathbf{x}}{\partial \xi}\cdot\left(\frac{\partial N_a}{\partial \eta}N_b - \frac{\partial N_b}{\partial \eta}N_a\right)d\xi d\eta$$
$$-\frac{1}{2}\int_A p\frac{\partial \mathbf{x}}{\partial \eta}\cdot\left(\frac{\partial N_a}{\partial \xi}N_b - \frac{\partial N_b}{\partial \xi}N_a\right)d\xi d\eta \tag{14}$$

in which a, b means the two different nodes in one element surface, N is the shape function.

For the two-dimensional problems, the description of the normal vector $\mathbf{n}$ is a lot simpler

$$\hat{\mathbf{n}}_e = \left\{ \begin{array}{c} -x_{2,\varepsilon} \\ x_{1,\varepsilon} \end{array} \right\} \tag{15}$$

the vector of stiffness coefficients is,

$$k_{p,ab} = \frac{1}{2}\int_L p\cdot\left(\frac{\partial N_a}{\partial \xi}N_b - \frac{\partial N_b}{\partial \xi}N_a\right)d\xi \tag{16}$$

5 Contact modeling

Without going into details, after spatial and temporal discretization, non linear problems involving contacts are governed by the following nodal algebraic equations defined at each time step :

$$F_i(U) + F_e(t) + F_c = 0 \tag{17}$$

where F_i is the vector of internal forces, F_e denotes the vector of external loads and F_c the vector of contact action/reaction forces. These equations are strongly non-linear with respect to the nodal displacements U, because of finite strains, large displacements of solids and the contact phenomenon (irreversibility of frictional effects).

A typical solution procedure for this type of non-linear analysis is obtained by using the Newton-Raphson iterative procedure :

$$\left\{ \begin{array}{l} K_T^i \Delta U = F + F_c \\ U^{i+1} = U^i + \Delta U \end{array} \right. \tag{18}$$

$K_T^i = -\frac{\partial F_i}{\partial U}$ is the tangential matrix (including mass and stiffness matrix) and $F = F_i(U_i) + F_e(t)$.

The gap vector between two bodies Ω_1 and Ω_2 in the global coordinates system is defined by :

$$X^{i+1} = U_{c1}^{i+1} - U_{c2}^{i+1} + X_0 \tag{19}$$

where U_{c1} (resp. U_{c2}) is the displacement vector of the contact node of Ω_1 (resp. Ω_2) and X_0 is the initial gap vector. The equation (19) can be easily transformed as follows :

$$X^{i+1} = CU^{i+1} + X_0 \tag{20}$$

where C is a condensation matrix.

By the virtual work principle, we have :

$$R^T \delta X = F_c^T \delta U \quad \Rightarrow \quad F_c = C^T R \tag{21}$$

where R represents the nodal contact forces in the global reference frame (X, Y, Z) . By combining equations (18), (20) and (21), we obtain :

$$X^{i+1} = W R + U_F \tag{22}$$

with

$$W = CK^{-1}C^T; \quad U_F = CK^{-1}F + CU^i + X_0 \tag{23}$$

Let Q be the rotation matrix between the local frame ($\mathrm{T}_1, \mathrm{T}_2, \mathrm{N}$) (Fig.2) and (X, Y, Z) . Let x and r be respectively the gap vector and the contact force vector in the local frame. Equation (22) may be written in the local frame :

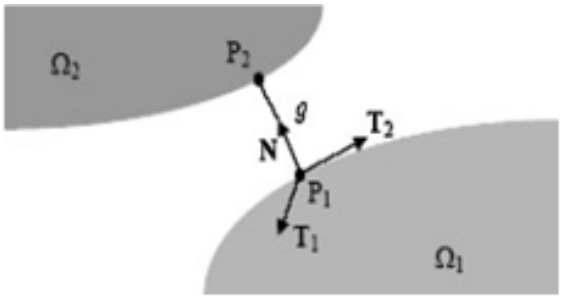

FIGURE 2 – The gap between two contact points

$$x = wr + x_f \tag{24}$$

where :$x = QX^{i+1}; r = QR; x_f = QX_f; w = Q^T WQ$.

For the following, let x_n be the algebraic value of the normal gap, x_t the tangential part of the gap vector, r_n the algebraic value of the normal contact force and r_t the tangential part of the contact force vector. The complete contact law (Signorini conditions + Coulomb friction laws) is a complex non-smooth dissipative law including three statuses :

$$\begin{array}{l} \text{Nocontact} : x_n > 0 \text{and} r = 0 \\ \text{Contactwithsticking} : \|x_t\| = 0 \text{and} r \in \text{int}(K_\mu) \\ \text{Contactwithsliding} : r \in bd(K_\mu) \text{with} r_t = -\mu r_n \frac{x_t}{\|x_t\|} \end{array} \tag{25}$$

where $\text{int}(K_\mu)$ and $bd(K_\mu)$ denote the interior and the boundary of the so-called coulomb cone respectively.

DeSaxcé and Feng [7] have proposed an augmented Lagrangian formulation of the contact derived from a bipotential function as follows :

$$r^* = r - \rho x^*;\ x^* = x + \mu \|x_t\| N \tag{26}$$

They have demonstrated that the three possible contact statuses as mentioned in Equation (25) can be stated from the following projection operator : if $r^* \in K_\mu$ (contact with sticking) then $r = r^*$, if $r^* \in K_\mu^*$ (separating) then $r = 0$ and if $r^* \in \mathbf{R}^3 - (K_\mu \cup K_\mu^*)$(contact with sliding) then r is the orthogonal projection of r^* onto K_μ . $K_\mu^*$is the polar cone of K_μ (Fig.3).

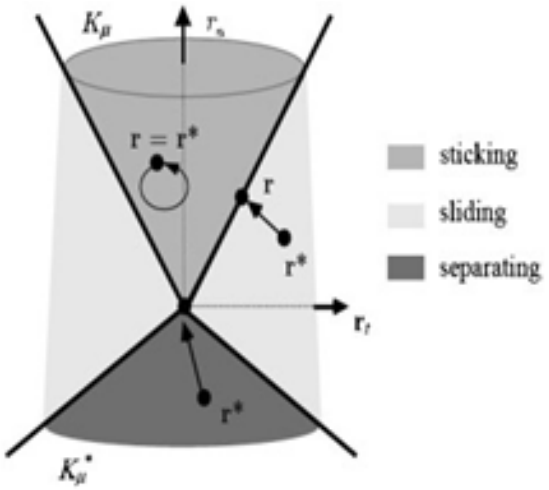

FIGURE 3 – The Coulomb cone and contact projection operators

Consequently, the projection operation can be explicitly defined by :

$$\begin{aligned}
&\mathrm{Proj}_{\mathrm{K}_\mu}(r^*) = r^* \text{ if } \|\mathrm{r}_\mathrm{t}^*\| < \mu r_n^* \\
&\mathrm{Proj}_{\mathrm{K}_\mu}(r^*) = 0 \quad \text{if } \mu\|\mathrm{r}_\mathrm{t}^*\| < -r_n^* \\
&\mathrm{Proj}_{\mathrm{K}_\mu}(r^*) = r^* - \left(\frac{\|r_t^*\| - \mu r_n^*}{1+\mu}\right)\left(\frac{\mathrm{r}_\mathrm{t}^*}{\|\mathrm{r}_\mathrm{t}^*\|} - \mu N\right) \text{ otherwise}
\end{aligned} \tag{27}$$

The contact solving problem is defined by :

$$\begin{cases} x = wr + x_f \\ r = \mathrm{Proj}_{\mathrm{K}\mu}(r^*) \end{cases} \tag{28}$$

where the unknowns are x and r. The solution can be done by using Uzawa or Newton techniques. Interested readers could find more details in[8].

6 Similation results and discussion

The problem concerns the muti-contact of three organs onto the pubis and pelvic floor due to the pressure. The organs are modelled by 2165 nodes and 1781 plane quadrilateral elements. We considered the pubis is constrained fully as a rigid body. The pelvic floor is constrained only in the two sides which obstruct the organs to expand from below. A uniform pressure is applied on the upper surfaces of rectum, uterus and bladder as shown in Figure 4.

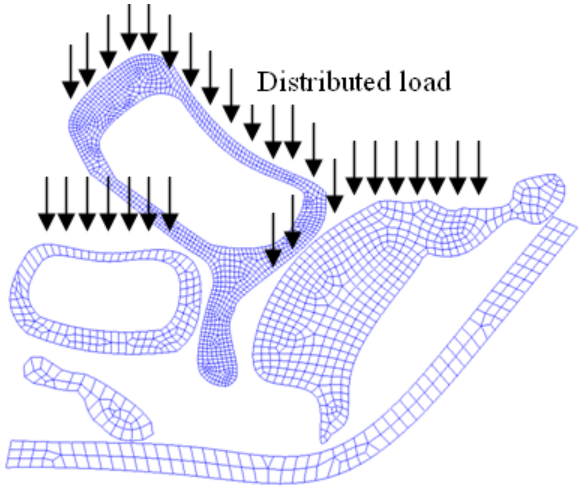

FIGURE 4 – Load application on pelvic system

Mooney-Rivlin constitutive law has been used in literature to model the behaviour of pelvic materials. Based on the linear elastic material properties of pelvic tissue (Poisson's ration=0.4, Young's modulus=15KPa [9]), the characteristics of this example are : C_{01} =2000Pa, C_{10} =500Pa, d =8000, mass density ρ = 500 kg/m3, pressure p =10Pa. The total simulation time is 3×10^{-3} s and the solution parameters are : Δt = 10^{-4} s, ξ = 0.5, θ = 0.55. We assume that no damping and Coulomb friction between contact surfaces exist. Fig.5 shows the distribution of the von Mises stress during the contact. It is noted that the concentration is localized in the contact zone as expected.

As we can see in figure 5, we have succeeded to simulate efficiently the interactions between these hyperelastic bodies due to the pressure. This is a first step which opens many perspectives and can propose a tool to help physicians to characterize functional impact of these organs. With this tool, it is possible to have a good idea of the impact force, the dimension of impact surface, the deepness of significant stresses, the energy absorbed by the soft tissue. Of course a lot of problems remain to be solved to have simulations close to reality as :

- having quantitative measurements of the mechanical properties of biological tissues in vivo.
- improving the modelling of soft tissue by building the 3D models with fine meshes, taking into account the internal pressures inside the organs which affects its deformation results.

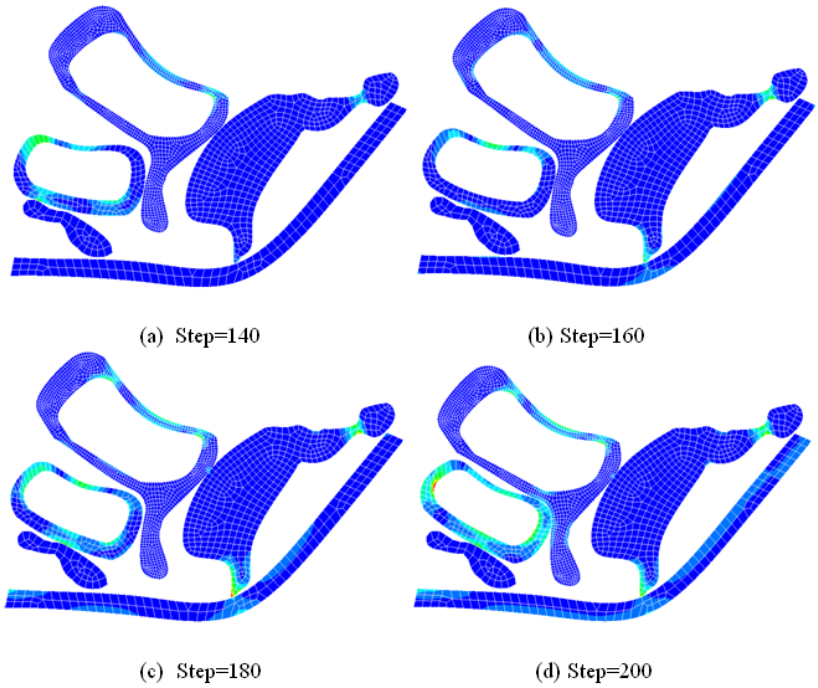

FIGURE 5 – Von-Mises stress distribution of four steps in one test

Références

[1] Olsen AL, Smith VJ, Bergstrom JO, Colling JC, and Clark A. Epidemiology of surgically managed pelvic organ prolapse and urinary incontinence. *Obstet Gynecol*, 89 :501–506, 1997.

[2] M. E. Bellemare, N. Pirró, L. Marsac, and O. Durieux. Toward the simulation of the strain of femal pelvic organs. In *EMBC07, 29th IEEE EMBS Annual international conference*, Lyon, France, August 23-26, 2007.

[3] Y.-C. Fung. *Biomechanics ; Mechanical Properties of Living Tissues*. Springer, Berlin, 1993.

[4] G.Venugopala Rao, Chrystèle Rubod, Mathias Brieu, Naresh Bhatnagar, and Michel Cosson. Experiment and finite element modelling for the study of prolapse in the pelvic floor system. *Comp. Methods in Biomechanics and Biomedical engineering*, 73 :317–330, 2008.

[5] Z.Q. Feng. http ://lmee.univ-evry.fr/∼feng/FerSystem.html, 2008.

[6] Javier Bonet and Richard D. Wood. *Nonlinear continuum mechanics for finite element analysis*. Cambridge University, United Kingdom, 1997.

[7] G. de Saxcé and Z.-Q. Feng. The bi-potential method : a constructive approach to design the complete contact law with friction and improved numerical algorithms. *Mathematical and Computer Modeling*, 28(4-8) :225–245, 1998.

[8] P. Joli and Z.-Q. Feng. Uzawa and Newton algorithms to solve frictional contact problems within the bi-potential framework. *Int. J. Numer. Meth. Engng.*, 73 :317–330, 2008.

[9] J. M. Hensel and et al. Development of multiorgan finite element-based prostate deformation model enabling registration of endorectal coil magnetic resonance imaging for radiotherapy planning. *Radiation Oncology Biol. Phys*, 68 :1522–1528, 2007.